Available online at www.sciencedirect.com
ScienceDirect
Journal of the European Ceramic Society 28 (2008) 1197–1203
www.elsevier.com/locate/jeurceramsoc

Structural and electrical characteristics of $LiNbO_3$ embedded in a 34% SiO_2 glass matrix

M.P.F. Graça [a,*], M.G. Ferreira da Silva [b], M.A. Valente [a]

[a] *Physics Department (I3N), Aveiro University, 3810-193 Aveiro, Portugal*
[b] *Glass and Ceramic Engineering Department (CICECO), Aveiro University, 3810-193 Aveiro, Portugal*

Received 28 June 2007; received in revised form 1 September 2007; accepted 8 September 2007
Available online 26 November 2007

Abstract

Lithium niobate ($LiNbO_3$) is a ferroelectric crystal and has attracted great attention due to its excellent piezoelectric, piroelectric, electrooptic, acustooptic and photorefractive properties. Recently, due to its electro-optical applications, a considerable interest has been shown in the preparation and study of its properties when embedded in a glass structure.

In this work, we present the preparation of the glass composition $34SiO_2$–$33Li_2O$–$33Nb_2O_5$ (mol%), by the melt-quenching method. The as-prepared sample, yellow and transparent, was heat-treated at 550, 575, 600 and 700 °C (HT) and at 575 °C with an electric field applied (thermoelectric treatment – TET). The applied electric fields were: (A) 100 kV/m; (B) 250 kV/m; (C) 500 kV/m. The glasses and glass-ceramics were studied by differential thermal analysis (DTA), X-ray power diffraction (XRD), scanning electron microscopy (SEM), dc conductivity (σ_{dc}), ac conductivity (σ_{ac}), dielectric and thermally stimulated depolarization current (TSDC) measurements.

$LiNbO_3$ crystal phase was detected, by XRD, in the samples treated without electric field applied, at temperatures above 575 °C. The increase of the electric field amplitude, applied during the thermal treatment, lead to the formation of a white layer in the sample surface in contact with the positive electrode during the heat-treatment. The σ_{dc}, σ_{ac} and the dielectric constant decrease with the rise of the treatment temperature. The presence of an electric field, during the HT process, seems to promote the growing of $LiNbO_3$ particles in a preferential crystal orientation, justifying the observed increase of the ε' values in the TET samples. The Z'' versus Z' plot shows a semi-arc for all samples, with the exception of the sample 600 HT whose Z'' frequency dependence is linear. The semi-arcs were fitted with a $R(R//\mathrm{CPE})(R_e//\mathrm{CPE}_e)$ equivalent circuit, using a CNLLS algorithm. The thermally stimulated depolarization current measurements show the presence of two depolarization current peaks in all HT samples.

The electrical and dielectrical behaviour, of the glass materials, shows the important role carried out by the heat-treatment conditions in the glass structure.

Keywords: $LiNbO_3$; Glass; Glass-ceramics; Structural properties; Electrical properties; Dielectrical properties

1. Introduction

The lithium niobate ($LiNbO_3$) crystal has been intensively studied in the last years due to a very attractive combination of large ferroelectric, piezoelectric, pyroelectric, photoelastic, electro and acustooptic and nonlinear optical properties. $LiNbO_3$ crystal has a rhombohedral lattice with $a = 5.492$ Å and $\alpha = 55.53$ Å. The Curie temperature of $LiNbO_3$ is 1210 °C and the spontaneous polarization is directed along the three-fold axis of symmetry.[1–3] As other ABO_3-type ferroelectric materials, $LiNbO_3$ has poor glass forming ability.[3] Thus, besides the extensive work on their physical properties and applications, very little study has been carried out in the formation of $LiNbO_3$ glasses or incorporation of $LiNbO_3$ crystals in glass networks. Knowing that the preparation of the $LiNbO_3$ crystals, using conventional routes (Czochralski process) is difficult and involves high costs, the possibility of preparing glass-ceramics with ferroelectric crystals has received considerable attention due to the ease of preparation and low costs, for getting dense materials allowing to control shape, size and distribution of the crystalline phase and thus, the properties of the glass-ceramic.[1,2]

* Corresponding author.
E-mail address: mpfg@ua.pt (M.P.F. Graça).

0955-2219/$ – see front matter © 2007 Elsevier Ltd. All rights reserved.
doi:10.1016/j.jeurceramsoc.2007.09.045

Due to the poor ability of $LiNbO_3$ for glass forming, the addition of a glass former is required for preparing glass-ceramics with $LiNbO_3$. Some works using SiO_2,[3–6] P_2O_5,[7–10] B_2O_3[11–14] and TeO_2[15–18] as glass formers in glass-ceramics with $LiNbO_3$ are available.

In this work, we use the SiO_2 as the glass former because its physical properties, and its role in glass forming are well-established[19] and because it is desirable that the glass former does not have cations that can modify the $LiNbO_3$ lattice. Silica satisfies these conditions because of its small ionic radius and coordination number.[4] Prasad et al.[4] show that for the SiO_2–Li_2O–Nb_2O_5 system, transparent and homogeneous glass can be obtained using a molar concentration of SiO_2 between 32% and 39% and the same concentration of Li_2O and Nb_2O_5. For this type of glass system, Todorovic and Radonjic[5] had verified that when the molar ratio $[Nb_2O_5]/[SiO_2] > 1$ and $[Li_2O] > 25\%$ transparent and homogeneous glasses are also obtained. In such glasses the use of a heat-treatment process allowed the formation of $LiNbO_3$ crystallites whose size increases with the rise of the HT temperature and time.

The present study describes the preparation of a $34SiO_2$–$33Li_2O$–$33Nb_2O_5$ (mol%) glass and glass-ceramics with $LiNbO_3$ particles, obtained by thermoelectric treatments. An attempt has been made to establish a correlation between the electrical properties of the glass and glass-ceramics, and their microstructure.

2. Experimental

A transparent glass with the molar composition $34SiO_2$–$33Na_2O$–$33Nb_2O_5$ was prepared by melt-quenching, using as raw materials: silicon oxide (SiO_2-BDH), sodium carbonate (Li_2CO_3-Merck) and niobium oxide (Nb_2O_5-Merck). The reagents, in appropriate amounts, were mixed for 1 h, in an agate ball-mixing planetary system. The mixture was heated in a platinum crucible at 700 °C, for 2 h, to remove the CO_2 from the Li_2CO_3, and melted at 1400 °C for 30 min. The molten material was quenched by pouring it into a stainless steel plate at room temperature and pressed by another plate to obtain flat samples with thickness of 10^{-3} m approximately. After that, the glass samples were annealed at 350 °C (during 3 h) to eliminate internal stresses, and then were slowly cooled inside the furnace (as-prepared sample).

To obtain glass-ceramics, the as-prepared sample was heat-treated (HT) in air, in a horizontal tubular furnace at 550, 575, 600 and 700 °C during 4 h. These temperatures were chosen in agreement with the differential thermal analysis results (DTA), carried out with a Linseis apparatus. A thermoelectric treatment (TET) process was performed in a vertical furnace where the as-prepared sample is pressed between two platinum electrodes connected to a high dc-voltage supply (PS325-SRS).[20] The TET has been done at 575 °C, during 4 h, with an external electric field of 100 kV/m (575A sample), 250 kV/m (575B sample) and 500 kV/m (575C sample).

The X-ray diffraction patterns were obtained at room temperature, using bulk samples, in a *Philips X'Pert* system, with a Kα radiation (λ = 1.54056 Å) at 40 kV, and 30 mA, with a step of 0.05° in 1 s. The samples microstructure was observed by scanning electron microscopy (SEM), performed in a *Hitachi S4100-1* system, on the free and fracture surface of carbon covered samples.

For the electrical measurements the opposite sides of the samples were painted with silver paste. The electrical dc conductivity (σ_{dc}) measurements and the thermally stimulated depolarization current (TSDC) were made using a Keithley 617 programmable electrometer as a function of the temperature. The σ_{dc} was measured between 200 and 370 K, in steps of 5 K. The accuracy of the temperature control and measurement is less than 0.1 K over the whole range. In this process, after the temperature become stable a dc voltage of 100 V was applied and 10 s later, the dc current measurement begins with 10 consecutive readings, in steps of 2 s. During these measurements, the samples were in a helium atmosphere, to improve the heat transfer and eliminate the moisture. The TSDC measurements were carried out, only for the samples heat-treated without an external electric field, using the following conditions: polarization temperature, 350 K; polarization time, 10 min; applied field, 100 kV/m; freezing temperature, 100 K; heating rate, 4°/min.[21] The impedance spectroscopy measurements ($Z^* = Z' - jZ''$) were carried out in the frequency range of 10 MHz–32 MHz using a *Solartron SI 1260*, *Impedance/gain-phase analyzer*.

The analytical background, used in the electrical data analysis, was as follows: (a) The ac and dc conductivities temperature dependence were fitted by an *Arrhenius* expression[4,22–24]; (b) The complex permittivity, $\varepsilon^* = \varepsilon' + j\varepsilon''$, was calculated through the sample impedance measurements: $Z^* = 1/(\mu\varepsilon^*)$ (where $\mu = j\omega C_0$, ω is the angular frequency, C_0 the capacitance of a vacuum (air) capacitor with plates identical to those formed by silver paint electrodes covering the flat-parallel surfaces of the samples and $j = \sqrt{-1}$).[22–24]

3. Results and discussion

The DTA result of the as-prepared sample shows the presence of exothermic peaks at 550 and 645 °C and thus the as-prepared sample was heat-treated at temperatures around this value. The Fig. 1 shows the XRD patterns for the samples HT at temperatures between 550 and 700 °C.

The heat treatments at temperatures above 600 °C make the samples opaque. This optical characteristic suggests the presence of crystallites in the glass matrix, which was confirmed by the XRD results (Fig. 1). The XRD pattern of the sample HT at 700 °C shows the additional presence of the $Li_2Si_2O_5$ crystal phase and was assigned to the 645 °C exothermic peak observed by DTA. However, the XRD pattern of the translucent 575HT sample already shows the presence of the $LiNbO_3$ crystal phase (Fig. 1). Fig. 2 shows the XRD patterns of the samples TET at 575 °C, where the $LiNbO_3$ crystalline phase is present. The rise of the number and intensity of the XRD peaks, comparing with the 575HT sample, indicates that the presence of the electric field makes easier the $LiNbO_3$ crystallization at lower temperatures than those required by the conventional heat-treatments.

The 575C sample surface (TET with 500 kV/m), which was in contact with the positive electrode during the TET, presents

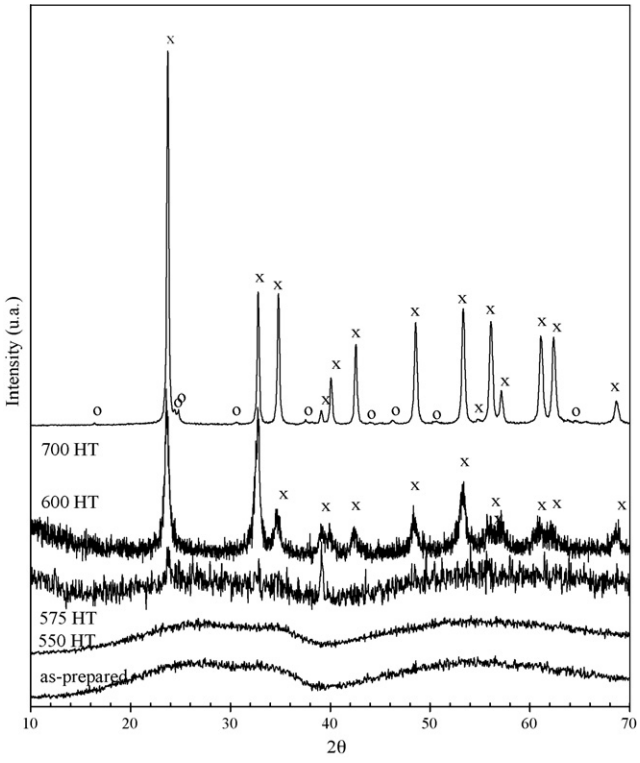

Fig. 1. XRD patterns of the HT samples ((×) $LiNbO_3$; (◯) $Li_2Si_2O_5$ in accordance with the JCPDS reference numbers 85-0504 and 72-0102, respectively).

a macroscopic white coating, with a thickness of ∼100 μm (Fig. 3d). The XRD patterns of the two opposite surfaces are identical, but the number of particles is larger in the surface that has been in contact with the positive electrode (Fig. 3). The SEM

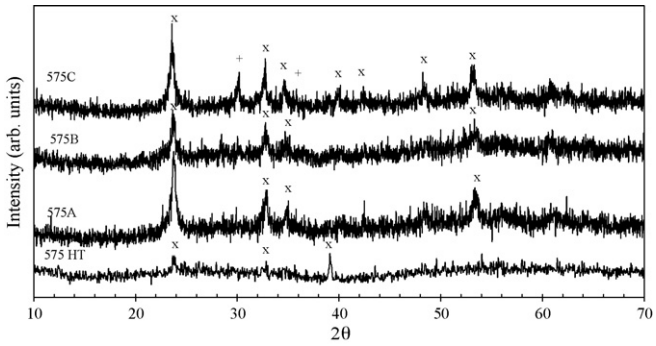

Fig. 2. XRD of the 575 °C TET samples ((×) $LiNbO_3$; (+) $LiNb_3O_8$ in accordance with the JCPDS reference numbers 01-085-0504 and 75-2154, respectively).

micrographs reveal that the rise of the electric field amplitude, used in the TET, increases the number of particles dispersed in the glass network. From the SEM micrographs, it was observed that, in the samples treated without external electric field, the number of particles inside the glass increase with the rise of HT temperature. An increase in the ratio between the crystallites volume and the glass matrix was also registered. In the fracture surface of these samples, the presence of particles was observed indicating that in this glass composition the crystallization occurs in volume. In the 575C TET sample, the $LiNbO_3$ and the $LiNb_3O_8$ crystal phases were detected (Fig. 2).

As mentioned, the increase of the HT temperature favours the increase of the volume ratio between the crystallites ($LiNbO_3$) and the glass matrix. This phenomenon implies a reduction of the number of ions structurally inserted in the glass as glass-modifiers (Li^+ and Nb^{5+}). The decrease of the quantity of these

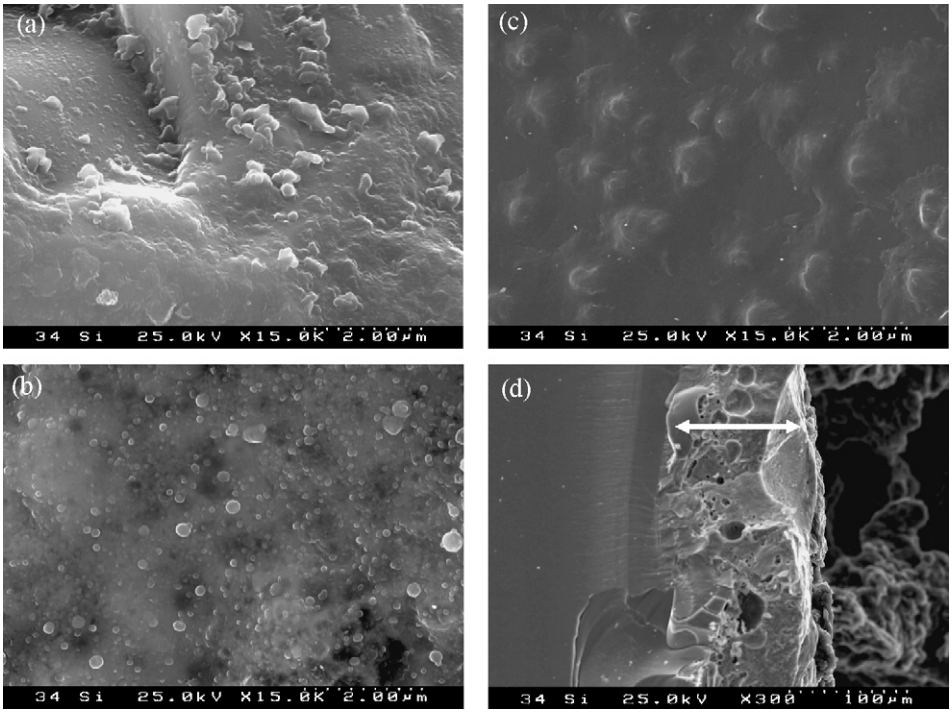

Fig. 3. SEM micrographs: (a) fracture surface of the 600 °C HT sample; (b) 575C sample surface, negative electrode; (c) 575C sample surface, positive electrode; (d) transversal section of the 575C, positive electrode (white coat).

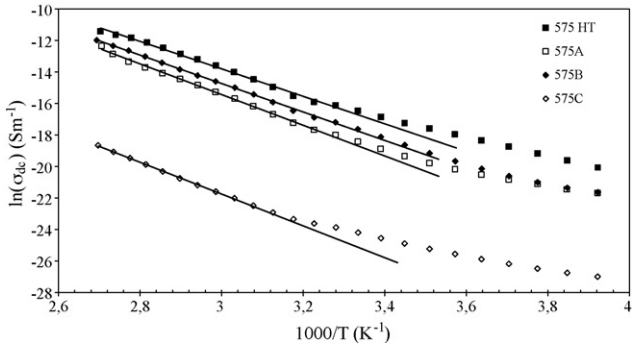

Fig. 4. $\ln(\sigma_{dc})$ versus $1000/T$ for the samples treated at 575 °C (the lines represent the theoretical fit).

ions can justify the observed reduction of the σ_{dc} from the as-prepared to the 600 °C HT sample (Table 1). It must be mentioned that the electrical and dielectrical properties of the sample HT at 700 °C were not studied due to the presence of the lithium disilicate crystal phase. In the TET samples, the rise of TET field amplitude until 250 kV/m (575B) leads to an increase of the $E_{a(dc)}$, suggesting a increase of the height of the potential barriers.[22–24] The 575B sample shows the highest σ_{dc} of all TET samples (Fig. 4; Table 1). Thus, this sample must present the highest number of charge carriers of all TET samples. The 575C sample has the lowest values of σ_{dc} and $E_{a(dc)}$. Besides the detection of the $LiNb_3O_8$ crystal phase, the presence on the surface in contact with the positive electrode of a white coat which is assigned to $LiNbO_3$ crystallites[20] should be responsible for the lower value of σ_{dc} due to the high resistivity of $LiNbO_3$ crystallites.[1] The presence of the electric field during the heat treatment increases the ion mobility and thus in the sample surface region in contact with the negative electrode the number of Li^+ ions structurally inserted as glass-modifiers, which have higher mobility than the Nb^{5+}, should increase with the rise of the external field amplitude. Therefore, the decrease of the number of Li^+ ions in the bulk region should promote the formation of $LiNb_3O_8$. These results show that the number of ions structurally inserted in the glass as glass-modifiers (Li^+ and Nb^{5+}) and the sample surface characteristics are the main parameters of this conduction process.

The decrease of the σ_{ac}, with the increase of the HT temperature (Fig. 5; Table 1), is due to the decrease of the number of

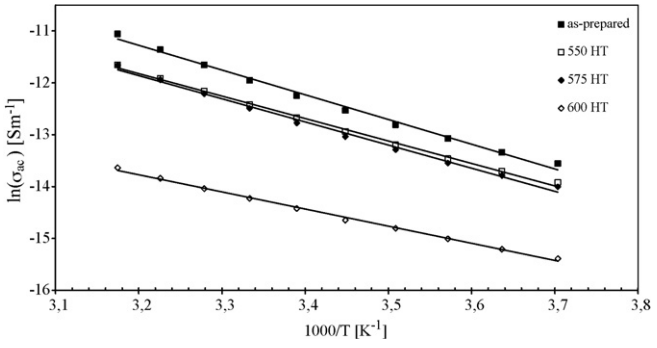

Fig. 5. $\ln(\sigma_{ac})$ versus $1000/T$ spectra of the as-prepared sample and HT samples (the line presents the theoretical fit).

Table 1
The dc conductivity (σ_{dc}) at 300 K, the dc activation energy ($E_{a(dc)}$), the ac conductivity (σ_{ac}), the ac activation energy ($E_{a(ac)}$), the dielectric constant (ε') and loss factor ($\tan\delta$) at 1 kHz and 300 K, the temperature of the TSDC peaks (P_1 and P_2) and the associated activation energy

Sample	σ_{dc} ($\times10^{-8}$) (Ω m)$^{-1}$	$E_{a(dc)}$ (kJ/mol)	σ_{ac} ($\times10^{-7}$) (Ω m)$^{-1}$	$E_{a(ac)}$ (kJ/mol)	ε'	$\tan\delta$	T_{P_1} (K)	E_a (kJ/mol)	T_{P_2} (K)	E_a (kJ/mol)
As-prep	37.50 ± 0.04	53.10 ± 0.59	64.60 ± 1.56	39.64 ± 1.13	69.00 ± 1.66	1.68 ± 0.06	216.4	44.62 ± 0.39	264.5	10.94 ± 0.15
550	11.61 ± 0.01	49.24 ± 1.11	40.51 ± 1.27	35.99 ± 0.69	60.95 ± 1.91	1.19 ± 0.05	222.4	45.83 ± 0.39	268	13.22 ± 0.39
575	7.08 ± 0.77	57.05 ± 1.38	37.62 ± 1.37	37.10 ± 1.02	54.10 ± 1.97	1.25 ± 0.06	220	35.81 ± 0.29	265	14.97 ± 0.10
600	0.179 ± 0.002	51.00 ± 3.34	6.62 ± 0.19	27.48 ± 0.53	39.89 ± 1.17	0.30 ± 0.01	249	40.56 ± 0.30	302.3	15.96 ± 0.29
575A	1.00 ± 0.01	58.39 ± 2.38	51.60 ± 1.59	41.22 ± 1.51	62.52 ± 1.92	1.49 ± 0.06				
575B	2.22 ± 0.03	61.95 ± 1.96	41.91 ± 1.77	36.10 ± 0.94	60.31 ± 2.56	1.25 ± 0.07				
575C	0.0032 ± 0.0004	51.69 ± 2.11	44.90 ± 1.14	36.45 ± 1.00	65.56 ± 1.67	1.23 ± 0.04				

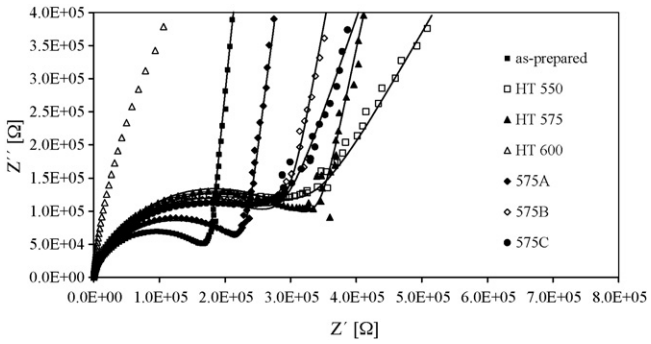

Fig. 6. Z'' versus Z' for all samples, measured at 300 K (the lines represent the theoretical fit).

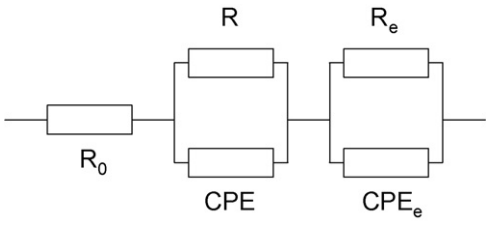

Fig. 7. The equivalent electric circuit model. R_0, R and R_e represent the high frequency sample resistance, the bulk resistance and the electrode associated resistance. CPE and CPE_e are constant phase elements associated with the bulk and electrodes, respectively.

mobile ions (glass-modifiers) and to the increase of the amount of $LiNbO_3$ crystallites, whose dipoles are hard to depolarize.[1] The $E_{a(ac)}$ (Table 1) was calculated through the $\ln(\sigma_{ac})$ versus $1/T$ dependence (Fig. 5) fitted by an Arrhenius expression. The decrease of the $E_{a(ac)}$ for the sample HT at 600 °C indicates that in this sample the electric dipoles have a larger mobility in following the ac electric field. However, this sample presents the lowest σ_{ac} (Table 1) showing that the number of dipoles, related with the ions structurally inserted in the glass as glass-modifiers (Li^+ and Nb^{5+}), is the main factor of this conductivity.

The number of electric dipoles, related with the modifier ions in the glass matrix and with the $LiNbO_3$ crystallites, are the main contributions to the dielectric constant (ε', Table 1). Nevertheless, in the samples treated without the external electric field the $LiNbO_3$ crystals observed in the surface and in the bulk region of the glass matrix probably do not present a preferential polar orientation. Thus, the random orientation of the $LiNbO_3$ crystallites leads to a decrease in the dipolar moment and thus the number of free ions structurally inserted in the glass as glass-modifiers represent the main contribution to ε'. In the 575 °C TET samples, their ε' value (Table 1) is larger than that of the sample treated without an external electric field applied. This behaviour suggests that the presence of the external electric field favours an increase of the number of $LiNbO_3$ crystals and promotes the crystal growth in a preferential direction. Thus, these samples show an increase in the dipole moment.

Fig. 6 shows the Cole–Cole plot using the Z^* formalism, for all samples, at 300 K. A quantitative characterization of the dielectric measurements was made using a complex non-linear least squares (CNLLS) algorithm associated with the Levenberg–Marquardt method.[6,10] This software adjusts the frequency dispersion data to an equivalent electric circuit model presented in Fig. 7, which is basically constituted by the parallel combination of polarization resistance (R) and constant phase element (CPE) of the sample (R//CPE) in series with the parallel combination of the R_e resistance and the CPE_e element, which are associated with the electrodes. R_0 (Fig. 7) corresponds to the sample resistance at high frequencies that was considered, by the algorithm, equal to zero. The impedance of this intuitive element can be defined by $1/Z_{CPE} = Q_0(j\omega)^n$ where Q_0 ($[Q_0] = Fs^{n-1}$) and n ($0 \leq n \leq 1$) are adjustable parameters independent of the frequency.[6,10,22–24]

All samples, with the exception of the HT600, present semi-arcs whose centers are below the Z'-axis, indicating the existence of a relaxation time distribution.[22–24] This behaviour must be related to the fact that in these systems the dielectric response depends on several components such as the glass matrix, the $LiNbO_3$ crystals, the dipoles related to the glass-modifier ions and the dipoles arising from the interface electrode-sample surface. It was verified that the low frequency range data can be theoretically adjusted with the R_e//CPE_e part of the electric equivalent circuit (Fig. 7). This indicates that these samples present a low frequency relaxation phenomenon. However, for lower frequencies (<100 Hz), the impedance measured data disperse due to sample-electrode interface polarization (Maxwell–Wagner phenomenon[22–24]) and thus the precision of the calculated R_e//CPE_e parameters is not enough to draw physical discussion. At higher frequencies (R//CPE parameters, Fig. 7), the Z^* fit results show that the parameter R diminishes, in all the samples, with the increase of the temperature of measurement, which is in agreement with the conductivity results. In all

Table 2
The parameters of the equivalent electric circuit

Sample	R//CPE				R_e//CPE_e		
	R ($\times 10^5$) (Ω)	Q_0 ($\times 10^{-8}$) [Ω^{-1} m^{-2} s^n]	n	τ_z ($\times 10^{-4}$) (s)	R_e ($\times 10^7$) (Ω)	Q_{0e} ($\times 10^{-7}$) (Ω^{-1} m^{-2} s^n)	n_e
As-prep	1.77	1.12	0.84	0.99	3.00	2.80	0.95
550	3.12	1.66	0.78	2.13	2.00	4.50	0.70
575	3.44	1.13	0.81	1.82	1.70	2.90	0.90
600							
575A	2.34	1.57	0.78	1.34	2.00	3.00	0.94
575B	3.01	1.47	0.79	1.91	1.80	1.80	0.92
575C	2.80	1.44	0.80	1.75	3.20	3.00	0.81

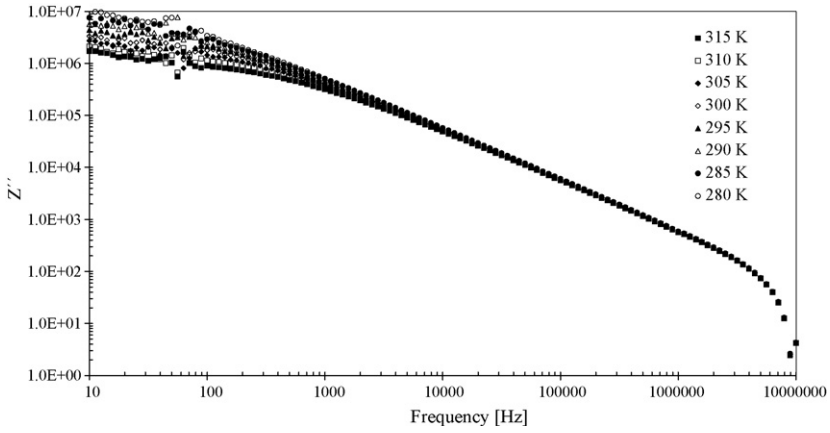

Fig. 8. Z'' versus frequency, in logarithmic scales, of the HT600 sample at several measurement temperatures.

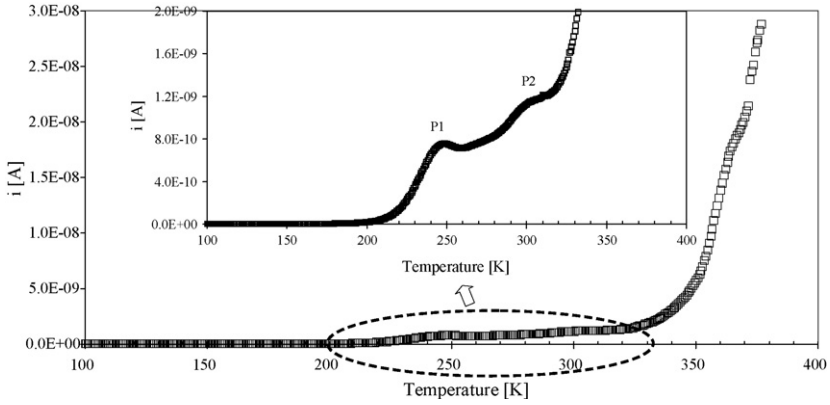

Fig. 9. TSDC spectra of the 600HT sample (the lines represent a theoretical adjust).

samples the n parameter, of the CPE element, is approximately 0.80 indicating a behaviour close to that of a capacitor element.

The dielectric relaxation time associated with the bulk response ($\tau_Z = 1/\omega_{(Z''\text{peak})}$[10,22–24]) (Table 2) decreases with the increase of the temperature of measurement, indicating an increase in the ability of the dipoles in following the electric field, which is in accordance with the σ_{ac}(T) spectra (Fig. 5).

The 600HT sample dielectric data can be fitted to the Curie–Von Schweidler formulation ($i(t) \propto t^{-s}$).[22–24] The inverse Fourier transform of this time dependence expression can lead to the expression $Z'' = kf^{-n}$, where Z'' is the imaginary part of the sample complex impedance, k a constant, f the frequency and n a fit parameter that can be related to the type of polarization.[22] Fig. 8 shows that the frequency dependence of Z'', for the 600HT sample, is linear indicating that in this frequency measurement range the sample does not present dielectric relaxations. We suggest that this behaviour can be associated to the lowest conductivity value (Table 1), observed in this sample, and thus a higher resistivity value. This indicates that the relaxation mechanism observed in the all other samples probably exists in the 600 HT sample but at a frequency higher than the upper limit of the equipment.

All samples present two TSDC peaks (Table 1). Fig. 9 illustrates the TSDC spectrum of the 600HT sample. In all samples the first TSDC peak (P_1), centred at temperatures below 240 K is, in agreement with Agarwall and Day,[25,26] due to the movements of the ions inserted structurally in the glass matrix. The P_2 peak, centred at temperatures >265 K, which presents an activation energy lower than the $E_{a(dc)}$ (Table 1), can be assigned to space-charge polarization that results from the movements of the charge carriers in limited paths that are due to the presence of micro-heterogeneities.[25,26] With the increase of the measuring temperature, for temperatures greater than the P_2 peak, it was observed, in all samples, an increase of the TSDC current showing an Arrhenius behaviour. The presence of TSDC peaks indicates the presence of low frequency dielectric relaxation mechanisms.

4. Conclusions

A transparent glass with the molar composition $34SiO_2$–$33Li_2O$–$33Nb_2O_5$ was prepared by the melt-quenching method. $LiNbO_3$ crystallites were formed in the glass by thermoelectric treatments of the as-prepared sample at treatment temperatures above 575 °C. The rise of the HT temperature increases the volume ratio between $LiNbO_3$ and the glass matrix and makes the samples opaque.

The presence of the electric field during the heating process favours the $LiNbO_3$ crystallization and the rise of the electric field amplitude increases the number of crystallites dispersed in

the glass network. The HT and TET process promotes the glass crystallization in volume.

The number of lithium and niobium ions inserted structurally in the glass network is the main parameter of these glass-ceramics conduction process. The analysis of the ε' value behaviour indicates that in the samples thermoelectric treated the $LiNbO_3$ crystals probably present a preferential polar orientation.

All the samples (with the exception of the 600HT, that does not present dielectric relaxations, in the used frequency measurement range) present, in the Z'' versus Z' plot, semi-arcs whose centres are under the Z'-axis, indicating the existence of a relaxation time distribution. These Z^* behaviour was adjusted to the $R(R//\text{CPE})(R_e//\text{CPE}_e)$ equivalent circuit.

The TSDC results show the presence of two current peaks (P_1 and P_2) assigned to: P_1 – local movements of free ions in the glass network between positions around the non-bridging oxygen (NBO) to which is bonded; P_2 – dipole depolarization from the charge carriers movements in limited paths, resulting from glass micro-heterogeneities and giving origin to space-charge polarization.

The TSDC theoretical fit indicates the existence of a larger number of relaxation processes. Thus the TSDC data must be described assuming the existence of a relaxation time distribution.

Acknowledgement

The authors thank to the FCT for the financial support (SFRH/BD/6314/2001).

References

1. Aboulleil, M. M. and Leonberger, F. J., Waveguides in lithium niobate. *J. Am. Ceram. Soc.*, 1989, **72**, 1311–1320.
2. Vogel, E. M., Glasses as nonlinear photonic materials. *J. Am. Ceram. Soc.*, 1989, **72**, 719–724.
3. Kim, J. E., Kim, S. J., Choi, H. W., Yang, Y. S. and Ohshima, Ken-ichi, Dielectric properties of $LiNbO_3$ glass mixed with strong glass former SiO_2. *J. Korean Phys. Soc.*, 2005, **46**(1), 52–54.
4. Prasad, E., Sayer, M. and Vyas, H. M., Li^+ conductivity in lithium niobate: silica glasses. *J. Non-Cryst. Solids*, 1980, **40**, 119–134.
5. Todorovic, M. and Radonjic, L., Lithium-niobate ferroelectric material obtained by glass crystallization. *Ceram. Int.*, 1997, **23**, 55–60.
6. Graça, M. P. F., Silva, M. G. F. and Valente, M. A., Dielectric and structural studies of a SiO_2–Li_2O–Nb_2O_5 glass and glass-ceramic prepared by the sol–gel method. *J. Non-Cryst. Solids*, 2005, **351**(33), 2951–2957.
7. Chou, K., Preparation of monolithic borophosphosilicate glass by the sol–gel method. *J. Non-Cryst. Solids*, 1989, **110**, 122–124.
8. de Araujo, E. B., de Paiva, J. A. C., de Araujo e, M. A. B. and Sombra, A. S. B., Crystallization of ferroelectric $LiNbO_3$ in niobophosphate glasses. *Phys. Scr.*, 1996, **53**, 104–107.
9. de Araujo, E. B., de Abreu, J. A. M., de Oliveira, R. S., de Paiva, J. A. C. and Sombra, A. S. B., Structure and electrical properties of lithium niobophosphate glasses. *Can. J. Phys.*, 1997, **75**, 747–758.
10. Graça, M. P. F., Valente, M. A. and Ferreira da Silva, M. G., The electric behavior of a lithium–niobate–phosphate glass and glass-ceramics. *J. Mater. Sci.*, 2006, **41**, 1137–1141.
11. Singh, K., Gandhi, P. R. and Chaudhari, B. M., Use of ferroelectric materials to modify cationic conduction of the Li_2O:B_2O_3 amorphous solid electrolyte system. *Solid State Ionics*, 1988, **28–30**, 752–755.
12. Huang, P. and Huang, X., The influence of MO_2, M_2O_5 and MO_3 oxides on the conductivity of lithium borate glasses. *Solid State Ionics*, 1989, **36**, 59–63.
13. Syam Prasad, N. and Varma, K. B. R., Evolution of ferroelectric $LiNbO_3$ phase in a reactive glass matrix ($LiBO_2$–Nb_2O_5). *J. Non-Cryst. Solids*, 2005, **351**, 1455–1465.
14. Venkatareman, B. H., Prasad, N. S., Varma, K. B. R., Rodriguez, V., Maglione, M., Vondermuhll, R. and Etourneau, J., Optical diffraction of second-harmonic signals in the LiBO–NbO glasses induced by self-organized LiNbO crystallites. *Appl. Phys. Lett.*, 2005, **87**, 091113.
15. Kim, H. G., Komatsu, T., Sato, R. and Matusita, K., Crystallization of $LiNbO_3$ in tellurite glasse. *J. Non-Cryst. Solids*, 1993, **162**, 201–204.
16. Kim, H. G., Komatsu, T., Sato, R. and Matusita, K., Incorporation of $LiNbO_3$ crystals into tellurite glasses. *J. Mater. Sci.*, 1996, **31**, 2159–2164.
17. Shankar, M. V. and Varma, K. B. R., Dielectric and optical properties of surface crystallized TeO_2–$LiNbO_3$ glasses. *J. Non-Cryst. Solids*, 1999, **243**, 192–203.
18. Ding, Y., Osaka, A. and Miura, Y., Stimulated surface crystallization of lithium niobate on tellurite glass due to ultrasonic treatment. *J. Non-Cryst. Solids*, 1994, **178**, 103–108.
19. Navarro, J. M. F., *El Vidrio*. CSIC-Fundación Centro Nacional del Vidrio, Madrid, 1991.
20. Graça, M. P. F., Silva, M. G. F., Sombra, A. S. B. and Valente, M. A., Electrical and dielectrical properties of SiO_2–Li_2O–Nb_2O_5 glass and glass-ceramics obtained by thermoelectric treatments. *J. Non-Cryst. Solids*, 2006, **352**, 5199–5204.
21. Fillard, J. P. and Van Turnhout, J., *Thermally Stimulated Processes in Solids: New Prospects*. Elsevier Scientific, 1977.
22. Jonscher, A. K., *Dielectric Relaxation in Solids*. Chelsea Dielectrics Press, London, 1983.
23. Kremer, F. and Schönhals, A., *Broadband Dielectric Spectroscopy*. Springer, Germany, 2002.
24. Ngai, K. L. and Rendell, R. W., *Handbook of Conducting Polymers*, *vol. II*. Marcel Dekker, N.Y., 1986.
25. Agarwal, A. K. and Day, D. E., Thermally stimulated currents and alkali-ion motion in silicate glasses. *J. Am. Ceram. Soc.*, 1982, **65**(2), 111–117.
26. Agarwal, A. K. and Day, D. E., Polarization and conduction mechanism in mixed-alkali glasses. *J. Am. Ceram. Soc.*, 1982, **65**(5), 231–237.